Pathway for the Transformation from Highly Oriented Pyrolytic Graphite into Amorphous Diamond

Keisuke Niwase,[1] Kazutaka G. Nakamura,[2] Manabu Yokoo,[2] Ken-ichi Kondo,[2] and Tadao Iwata[3,4]
[1]*Hyogo University of Teacher Education, Kato, Hyogo 673-1494, Japan*
[2]*Materials and Structures Laboratory, Tokyo Institute of Technology, 4259 Nagatsuta, Yokohama, 226-8503, Japan*
[3]*Nuclear Professional School, School of Engineering, University of Tokyo, Tokai, Ibaraki 319-1188, Japan*
[4]*Japan Atomic Energy Research Institute (JAERI), Tokai, Ibaraki 319-1195, Japan*

(Received 5 October 2008; published 20 March 2009)

We report the discovery of a novel pathway for the transformation from highly oriented pyrolytic graphite foils into amorphous diamond platelets. This pathway consists of three stages of neutron irradiation, shock compression, and rapid quenching. We obtained transparent platelets which show photoluminescence but no diamond Raman peak, similar to the case of amorphous diamond synthesized from C_{60} fullerene. Wigner defects formed by irradiation are considered to make a high density of diamond nucleation sites under shock compression, of which growth is suppressed by rapid quenching.

DOI: 10.1103/PhysRevLett.102.116803 PACS numbers: 81.05.Uw

Irradiation of high energy particles is known to induce modifications of materials such as cross-linkings of polymers [1]. Recently, cross-linking defects were suggested to be formed in irradiated graphite [2] and carbon nanotubes [3], giving insights on the so-called Wigner defects which have been a long time issue as they induce an undesirable effect on atomic reactors [4,5]. The transformation from graphite to diamond, on the other hand, is also a long time issue [6], and polycrystalline diamond of 10–20 nm across, which exhibits an excellent hardness, was recently synthesized by direct conversion of graphite under static high pressure and temperature [7]. The ultimate smallest crystalline size of diamond was synthesized from C_{60} fullerene by the shock compression and rapid quenching (SCARQ) technique [8,9], which is a unique method to obtain metastable carbon materials, transformed from the initial carbon phase in a flash. The obtained material is transparent and comprised wholly of sp^3 carbon, suggesting diamond structure, but the diamond crystalline size is within the range of a unit cell. Then it was labeled "amorphous diamond" as it is amorphous in the long-range order and diamond in the short-range order [10]. Graphite has not been found to transform to amorphous diamond by shock compression but to crystalline diamond by the martensitic mechanism [11], if shock pressure is applied parallel to the c axis. Here we show a transformation from highly oriented pyrolytic graphite to transparent amorphous diamond tiles by SCARQ. Preirradiation of graphite with a high energy neutron is the key to success.

We utilized highly oriented pyrolytic graphite (HOPG) of HOPG-ZYA from Union Carbide as a starting material and irradiated with fast neutrons at about 333 K to a dose of $2.6 \times 10^{24} n\ \mathrm{m}^{-2}$ ($E > 1$ MeV) in the JAERI JRR-2 nuclear reactor. Displacement per atom (DPA) for the neutron-irradiated specimen is estimated to be about 0.2 DPA [12]. The thermal conductivity of the sample at room temperature was reduced to less than $1/100$ of that of the unirradiated one [13]. Thin films of about 8 μm in thickness were prepared by cleavage with a razor for the unirradiated and irradiated HOPG specimens. Optical microscopy showed that the cleaved surface of the irradiated specimen still remained in a flat and shinning state. The sample was sandwiched by gold foils (200 μm thick), which work for heat sinks, and inserted in an iron capsule, in which thickness of the front and back wall of the capsule was 2.5 and 3.0 mm, respectively. The tungsten flyer (2 mm thick and 19.5 mm in diameter) was accelerated to 1.70–1.72 km/s by a powder gun and was impacted to the front side of the iron capsule. The shock pressures determined by the flyer velocity were 51 and 52 GPa for the neutron-irradiated and the original specimen, respectively. The shock pressure was estimated with impedance matching between tungsten and iron, where the effect of the thin gold foils was neglected. The shock wave propagated parallel to the c axis of HOPG and shock duration was estimated to be 540 ns. The estimated shock temperature of the sample was 3800 K by the first shock and approximately 2000 K during the shock duration. The shocked sample was recovered from the capsule. Raman spectra were obtained by a Raman microscope (SPEX, RAMAN-500-UVR). 488 nm light from an Ar-ion laser was focused on the sample with a 40× objective and a power of 20 mW, which is low enough to avoid some laser irradiation-induced annealing.

Figure 1 shows scanning electron micrographs [(a) and (b)] and optical micrographs [(c) and (d)] of the neutron-irradiated sample recovered after the shock compression and rapid quenching. A part of the gold foil of the sandwiched specimen was stripped to investigate the recovered sample. We find divisions of the dark areas by bright lines [Fig. 1(a)], which correspond to an occurrence of fracture of the original specimen into tiles. The size of tiles ranged from several micrometers to several tens of micrometers.

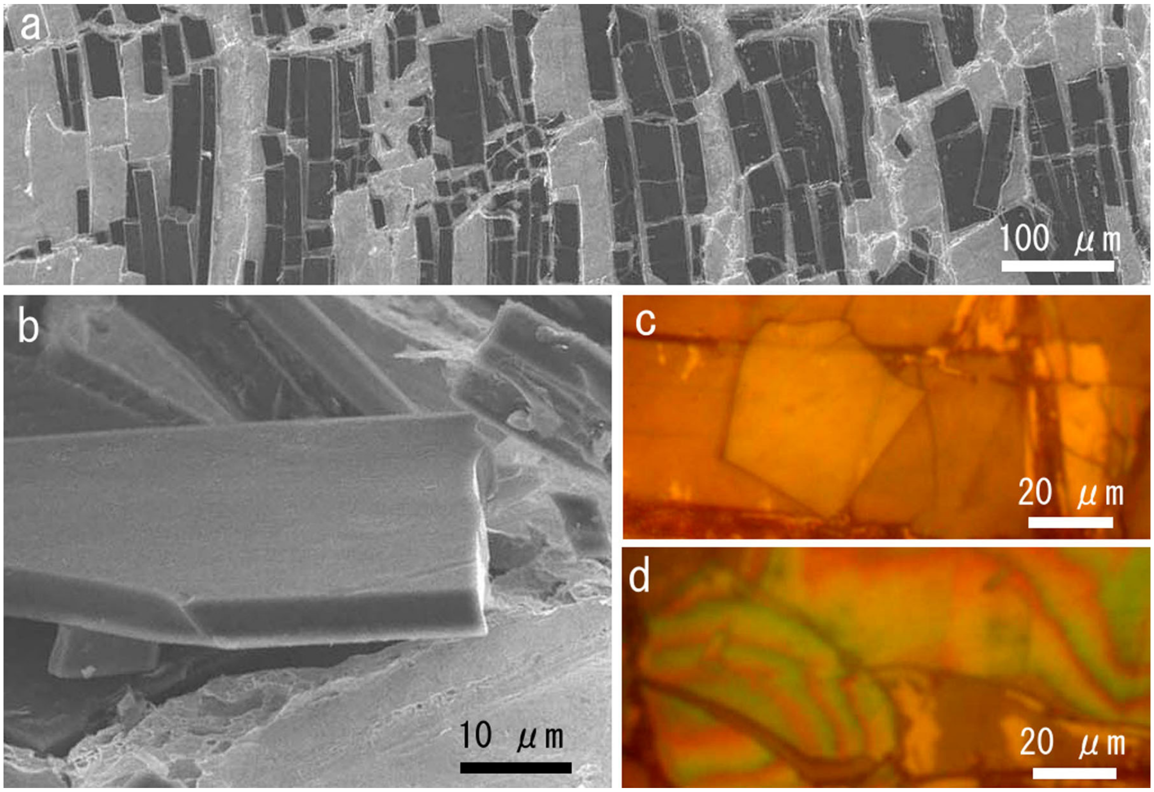

FIG. 1 (color online). Electron and optical micrographs of neutron-irradiated HOPG recovered after the shock compression and rapid quenching. (a) Dark and bright areas correspond to the original graphite area and the gold foil, respectively. Division of the dark areas by bright lines indicates an occurrence of a fracture of the specimen into tiles. Some of the tiles were stripped off, exposing the gold foil surface. (b) An oblique view of a tile. The cross section of the tile is seen to be homogeneous, implying a disappearance of the initial layered structure of graphite along the *c* axis. (c) A tile riding on fractured tiles. The tile is optically transparent, and then splitting lines below the tile can be seen. (d) Interference patterns observed for transparent tiles.

Similar fractures have been observed for the C_{60} fullerene samples recovered after the shock compression [9,14]. An oblique view of the tile reveals uniformity along the *c* axis and absence of the initial layered structure of graphite [Fig. 1(b)]. Tiles are optically transparent [Figs. 1(c) and 1(d)] and stable under ambient conditions such as air and light.

Figure 2 compares the Raman spectra for the unirradiated HOPG, the neutron-irradiated HOPG, and the neutron-irradiated HOPG recovered after the shock compression. The Raman measurements were done in the same condition to compare the relative intensity. The original HOPG specimen shows a sharp graphite peak at 1580 cm^{-1} on E_{2g} mode. After neutron irradiation, the graphite peak disappeared, and then a broad band ranging from 800 to 1700 cm^{-1} appeared, of which shape is similar to amorphous carbon consisting mostly of sp^2 bondings [15]. After the shock compression, a dramatic change occurred in the Raman spectrum. We observe two broad bands at 1600 and 2300 cm^{-1} and a remarkable increase of the background intensity. No diamond peak at around 1332 cm^{-1} is observed in spite of the transparency. The broad band at 2300 cm^{-1} changes the position depending on tiles, and then it should be originated in the interference of laser beams reflected from the top and the bottom of the transparent tiles that is directly seen in the optical image of Fig. 1(d). The increase of the background intensity has been seen for the amorphous diamond synthesized from C_{60} fullerene by shock compression and is due to photoluminescence, probably originating in an existence of defective sp^3 bondings [14]. One should note that the broad band at about 1600 cm^{-1} did not appear for the amorphous diamond synthesized from C_{60} fullerene but did for the polymerized C_{60} fullerene formed by a lower shock pressure [14]. This suggests that the transition to amorphous diamond is not complete in the present case with some remaining sp^2 bondings.

Another shock compression and rapid quenching experiment was done with unirradiated HOPG in the same pressurized condition to confirm the irradiation-induced defects on the transformation. The result was completely different from the irradiated one. After the shock compression, the unirradiated HOPG foil was broken into pieces with jagged edges and a remaining layered structure (Fig. 3). Optically, the specimen remained in the initial shiny state. Raman spectroscopy shows the original graphite peak at 1580 cm^{-1} and an additional defect peak at 1355 cm^{-1}. This implies a reduction of the crystalline size

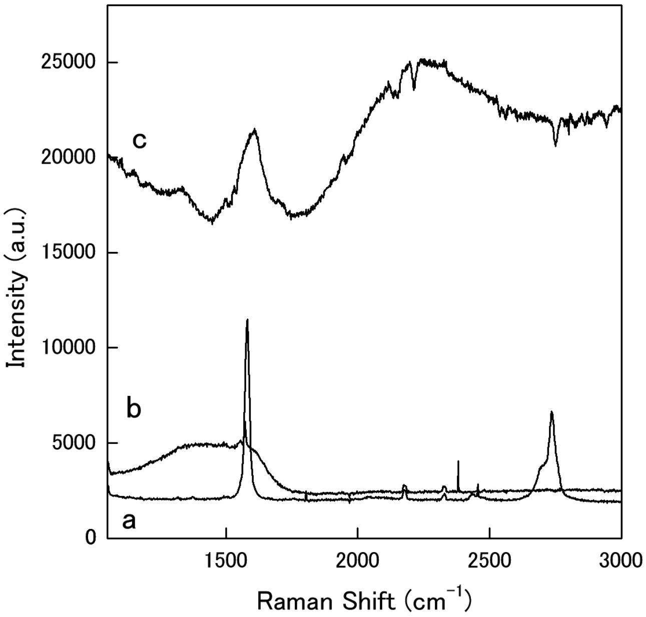

FIG. 2. Raman spectra for the original and neutron-irradiated HOPG specimens and a change of the Raman spectrum for the irradiated one after the shock compression. (a) Spectrum of the original HOPG showing the first-order band (*G* band) near 1580 cm^{-1} and the second-order Raman band near 2700 cm^{-1}. (b) Spectrum of the neutron-irradiated HOPG showing a broad band in a range from 800 to 1700 cm^{-1}. The original *G* band and the second-order Raman band mostly disappeared. (c) Representative spectrum of the neutron-irradiated HOPG after the shock compression showing broad bands near 1600 and 2200 cm^{-1} and a remarkable increase of the background intensity.

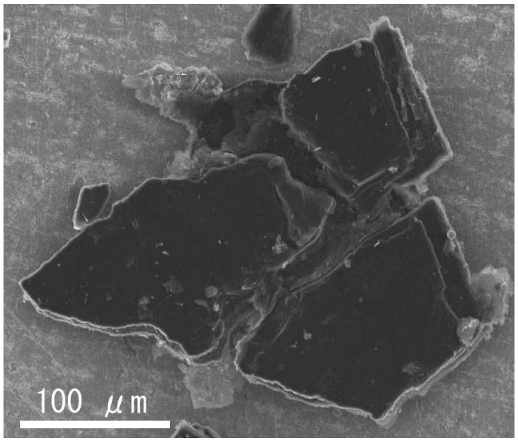

FIG. 3. Electron micrograph of HOPG specimen recovered after the shock compression. The shock experiment was done in almost the same pressurized condition done for the neutron-irradiated HOPG. The specimen is broken into pieces with jagged edges but still preserves the initial layered structure.

of graphite [16] from the initial crystalline size of 20 μm after the shock compression.

The clear difference in the nature of recovered specimens indicates a significant effect of irradiation-induced defects on the synthesis of amorphous diamond by SCARQ. Disordered carbon forms have been shown to be preferable as the starting materials to minimize the pressure and temperature conditions of diamond synthesis for both shock compression [17,18] and multianvil experiments [19]. The presence of defects such as crystal surface termination, sp^3 hybridized bonds, and higher molar volume (low density) of those materials is suggested to relate the nucleation of diamond [19].

A question arises: What kinds of irradiation-induced defect should play an important role on the transformation in the present case? The irradiation effects on graphite have been investigated by many researchers as they are an important issue on graphite moderators of a nuclear reactor [20–28]. High energy particles passing through graphite lattice may cause the displacement of atoms. If the energy transferred to an atom in the lattice is larger than the displacement threshold energy, the atom is pushed into the lattice to form an interstitial, leaving a vacancy behind, which is called a Frenkel pair. Interstitials and vacancies, respectively, develop to various types of defect clusters under irradiation. Frenkel pairs remaining after irradiations remarkably annihilate on annealing above 573 K, releasing Wigner energy [21–23,26]. According to the experimental [20–30] and theoretical studies [2,31,32], the irradiation-produced defects can be classified into in-plane defects of single vacancy, vacancy clusters and dislocation dipoles, single interstitial, interstitial clusters such as di-interstitials, and cross-linking defects, as shown in Fig. 4. A dislocation dipole is considered to be a reconstructed vacancy line cluster with a pair of sevenfold and fivefold rings or an eightfold ring at the ends [31]. The formation of these defects depends on the irradiation temperature, dose, and incident particles. Under prolonged irradiation, disordering occurs preferentially in the basal planes of graphite by the accumulation of dislocation dipoles [31], which would induce the buckling and rotation of basal planes [25,30]. The disordered structure is thermally stable on annealing at 873 K [23].

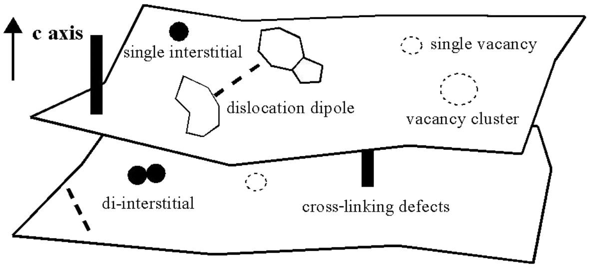

FIG. 4. Irradiation-produced defects proposed by recent experimental and theoretical studies. Interlayer defects of single interstitial, interstitial clusters such as di-interstitials, and cross-linking defects are presented in the figure. Dislocation dipoles with an eightfold ring or a pair of sevenfold and fivefold rings at the ends should induce the disordering of graphite by the buckling and rotation of the basal plane.

The broad Raman spectrum of the neutron-irradiated graphite (Fig. 2) is generally considered to be a signal of amorphous carbon [15,24,27]. However, one should note that we could cleave the neutron-irradiated HOPG parallel to the basal plane. This supports the preferential disordering of the basal planes and suggests the number of cross-linking defects is not so high as to strongly combine the neighboring planes. Also, we should note that the irradiated HOPG is already compressed locally by the existence of irradiation-induced defects. The *a* spacing decreases by about 2%, which induces the softening of the out-of-lane vibrations [33], while the *c* spacing expands by more than 15%.

A tentative scenario on the synthesis of amorphous diamond tiles from the neutron-irradiated HOPG under shock compression is as follows. The disordered layered sequences [27,30,31] induced mainly by the formation of dislocation dipoles prevent the martensitic transformation from graphite to diamond under shock compression. Defective sites relating to Wigner defects should make a high density of diamond nucleation sites, leading to the synthesis of amorphous diamond tiles, although the dominant defect for the nucleation is still an open question. The release of Wigner energy of about 3 kJ/g, and the softening of the out-of-plane vibrations may assist to conquer the transition barrier on the bonding change from sp^2 to sp^3 in the pressurized condition.

In conclusion, we have discovered a novel pathway for the transformation from highly oriented pyrolytic graphite into amorphous diamond. The pathway consists of neutron irradiation, shock compression, and rapid quenching. Wigner defects produced by irradiation are considered to work as the nucleation sites for diamond. In the pathway, we can control the introduction of Wigner defects in terms of the kind, the amount, and the spatial distribution by changing the irradiation condition of dose, temperature, and incident species [20–32,34] and preparing thin foils by cleavage as a starting material for the shock compression. Thus, the combined method of irradiation and shock compression is a promising way to synthesize new carbon materials such as amorphous diamond. Further experimental and theoretical studies are needed to clarify the transition mechanism with the aid of Wigner defects and the detailed properties of amorphous diamond generated from graphite.

---

[1] A. Charlesby, Nature (London) **171**, 167 (1953).
[2] R. H. Telling, C. P. Ewels, A. El-Barbary, and M. I. Heggie, Nature Mater. **2**, 333 (2003).
[3] K. Urita, K. Suenaga, T. Sugai, H. Shinohara, and S. Iijima, Phys. Rev. Lett. **94**, 155502 (2005).
[4] E. P. Wigner, J. Appl. Phys. **17**, 857 (1946).
[5] E. W. J. Mitchell and M. R. Taylor, Nature (London) **208**, 638 (1965).
[6] F. P. Bunday, H. T. Hall, H. M. Strong, and R. H. Wentorf, Jr., Nature (London) **176**, 5 (1955).
[7] T. Irifune, A. Kurio, S. Sakamoto, T. Inoue, and H. Sumiya, Nature (London) **421**, 599 (2003).
[8] C. S. Yoo, W. J. Nellis, M. L. Sattler, and R. G. Musket, Appl. Phys. Lett. **61**, 273 (1992).
[9] H. Hirai, K. Kondo, N. Yoshizawa, and M. Shiraishi, Appl. Phys. Lett. **64**, 1797 (1994).
[10] H. Hirai, Y. Tabira, K. Kondo, T. Oikawa, and N. Ishizawa, Phys. Rev. B **52**, 6162 (1995).
[11] D. J. Erskine and W. J. Nellis, Nature (London) **349**, 317 (1991).
[12] T. Iwata and T. Nihira, J. Phys. Soc. Jpn. **31**, 1761 (1971).
[13] T. Nihira and T. Iwata, in *Point Defects and Defect Interactions in Metals*, edited by J. Takamura, M. Doyama, and M. Kiritani (University of Tokyo, Tokyo, 1982) pp. 236–238.
[14] K. Niwase, T. Homae, K. G. Nakamura, and K. Kondo, Physica (Amsterdam) **376B–377B**, 280 (2006).
[15] A. C. Ferrari and J. Robertson, Phil. Trans. R. Soc. A **362**, 2477 (2004).
[16] F. Tuinstra and J. L. Koenig, J. Chem. Phys. **53**, 1126 (1970).
[17] H. Hirai, S. Kukino, T. Ohwada, and K. Kondo, J. Am. Ceram. Soc. **78**, 2079 (1995).
[18] K. Yamada and Y. Tanabe, Carbon **40**, 261 (2002).
[19] C. L. Guillou, F. Brunet, T. Irifune, H. Ohfuji, and J. Rouzaud, Carbon **45**, 636 (2007).
[20] R. A. Thrower, in *Chemistry and Physics of Carbon*, edited by P. L. Walker, Jr. (Dekker, New York, 1969), Vol. 5, p. 217.
[21] B. T. Kelly, *Physics of Graphite* (Applied Science, London, 1981).
[22] T. Iwata, J. Nucl. Mater. **133–134**, 361 (1985).
[23] K. Niwase, T. Tanabe, and I. Tanaka, J. Nucl. Mater. **191–194**, 335 (1992).
[24] M. S. Dresselhaus and R. Kalish, *Ion Implantation in Diamond, Graphite and Related Materials* (Springer-Verlag, Berlin, 1992).
[25] T. Tanabe, S. Muto, and K. Niwase, Appl. Phys. Lett. **61**, 1638 (1992).
[26] E. Asari, M. Kitajima, K. G. Nakamura, and T. Kawabe, Phys. Rev. B **47**, 11 143 (1993).
[27] K. Niwase, Phys. Rev. B **52**, 15 785 (1995); **56**, 5685 (1997).
[28] Z. Tang, M. Hasegawa, T. Shimamura, Y. Nagai, T. Chiba, Y. Kawazoe, M. Takenaka, E. Kuramoto, and T. Iwata, Phys. Rev. Lett. **82**, 2532 (1999).
[29] A. Hashimoto, K. Suenaga, A. Gloter, K. Urita, and S. Iijima, Nature (London) **430**, 870 (2004).
[30] A. Asthana, Y. Matsui, M. Yasuda, K. Kimoto, T. Iwata, and K. Ohshima, J. Appl. Crystallogr. **38**, 361 (2005).
[31] K. Niwase, Philos. Mag. Lett. **82**, 401 (2002); Mater. Sci. Eng. A **400–401**, 101 (2005).
[32] L. Li and J. Robertson, Phys. Rev. B **72**, 184109 (2005).
[33] T. Nihira and T. Iwata, Phys. Rev. B **68**, 134305 (2003).
[34] M. Saito, K. Yamashita, and T. Oda, Jpn. J. Appl. Phys. **46**, L1185 (2007).